PERGAMON

International Journal of Heat and Mass Transfer 43 (2000) 3359–3370

International Journal of HEAT and MASS TRANSFER

www.elsevier.com/locate/ijhmt

Experimental study of unsteady thermal convection in heated rotating inclined cylinders

David Lin, Wei-Mon Yan*

Department of Mechanical Engineering, Huafan University, Shih Ting, Taipei, Taiwan 22305

Received 30 April 1999; received in revised form 16 November 1999

Abstract

An experimental study through temperature measurements was conducted to investigate the thermal characteristics induced by the interaction between the thermal buoyancy and rotation-induced Coriolis force and centrifugal force in an air-filled heated inclined cylinder rotating about its axis. Results were obtained for the following ranges of the governing groups: thermal Rayleigh number $Ra = 2.3 \times 10^6$ and 4.6×10^6, Taylor number $0 \leq Ta \leq 2.2 \times 10^{10}$, rotational Rayleigh number $0 \leq Ra_\Omega \leq 5.9 \times 10^8$ and inclined angle $0 \leq \Psi \leq 90^\circ$. The experimental data suggested that when the cylinder is stationary, the thermal buoyancy driven flow is random oscillation at small amplitude after initial transient for inclined angle $\Psi < 60^\circ$. Rotating the cylinder was found to destabilize the temperature field when the rotation speed Ω is less than 30 rpm and to stabilize it when the Ω exceeds 30 rpm. Additionally, the distributions of time-average temperature θ_{av} in the Z-direction for various inclined angles become widely separate only at low rotation rates, $\Omega < 60$ rpm.

1. Introduction

If a heated enclosure undergoes rotation, centrifugal and Coriolis force effects on the fluid will interact with the gravitational force in a manner which results in a complex three-dimensional flow and temperature fields. The flow and temperature fields are directly coupled in the momentum equations, and this consequently effects the wall heat transfer rates. Analysis of flow and heat transfer associated with rotating systems is quite complex due to the simultaneous influence of centrifugal and Coriolis forces. As a consequence, a large amount of analytic and experimental study has been and continues to be devoted for the development of a general treatment of the influence of rotation on the flow and heat transfer in simple geometries. However, the details on how these interactive forces act on the complex resulting flow are still poorly understood. In this respect, it is further required that the detailed experimental study has to be conducted in order to provide information on the flow and heat transfer characteristics.

The objective of this work is to present a systematic experimental study to investigate the thermal characteristics due to the interaction between the gravitational field and the rotational induced body forces in an air-filled heated cylinder rotating about its inclined axis with a constant angular velocity. As would be anticipated, the influence of the centrifugal and Coriolis forces arising from the rotation will affect significantly the flow and heat transfer characteristics of natural convection. Emphasis will be cen-

* Corresponding author. Tel.: +886-2-2663-3847; fax: 886-2-2663-3847.

E-mail addresses: david@huafan.hfu.edu.tw (D. Lin), wmyan@huafan.hfu.edu.tw (W.-M. Yan).

0017-9310/00/$ - see front matter
PII: S0017-9310(99)00380-4

Nomenclature

D	cylinder diameter (m)
g	gravitational acceleration (m/s^2)
H	cylinder height (m)
k	thermal conductivity (W/m K)
Pr	Prandtl number, ν/α
r, z	dimensional coordinate system
R, Z	dimensionless coordinate system, $R = r/D$, $Z = z/D$
Ra	thermal Rayleigh number, $g\beta\Delta TD^3/\alpha\nu$.
Ra_Ω	rotational Rayleigh number $\Omega^2 D\beta\Delta TD^3/\alpha\nu$
t	time (s)
T	temperature ($^\circ C$, K)
Ta	Taylor number, $\Omega^2 D^4/\nu^2$
T_H	temperature of the hot (bottom) wall (°C, K)
T_L	temperature of the cold (top) wall (°C, K)
T_0	initial fluid temperature, $T_0 = (T_H + T_L)/2$

Greek symbols

α	thermal diffusivity (m^2/s)
β	thermal expansion coefficient (1/K)
γ	aspect ratio, H/D
ΔT	temperature difference between the hot and cold walls (°C, K)
θ	dimensionless temperature, $(T - T_L)/\Delta T$
θ_{av}	time-average temperature
Ψ	inclined angle of cylinder
ν	kinematic viscosity (m^2/s)
ρ	density (kg/m^3)
τ	dimensionless time, $t/(D^2/\alpha)$
Ω	angular speed

Subscripts

av	average
H	hot wall
L	cold wall
ref	condition at reference condition

tered on the local temperature measurement. This class of rotating flow geometry may lead to a new area of experimental research, to supplement the available information of natural convection in confined cylinders, in addition to numerous future applications in Bridgman melt growth, spacelab, and design development in cooling rotating equipments.

The general purpose of the following literature survey is to present the main features of heat transfer and flow pattern in rotating fluid systems. Concerning about the rotating cavities, quite early studies were interested in the rotating Rayleigh–Benard convection [1–7], that is, the convection in an infinite bounded horizontal layer of fluid subject to an unstable vertical temperature gradient, which rotates at constant angular speed about a vertical axis. Based on the linear stability analysis, Niller and Bisshopp [1] concluded that for large Taylor number Ta, the viscous effects play an important role in a thin layer near the boundary. Numerical analysis performed by Veronis [2] found that for Prandtl number $> \sqrt{2}$, the velocity and temperature fields were dominated by the rotational constraint even for moderate values of Taylor number (10^3). For the limit of infinite Prandtl number, Kuppers and Loetz [3] showed that no stable steady-state convective flow exists if the Taylor number exceeds certain critical value. An extensive and detailed study of Benard convection stability with and without rotation was performed by Rossby [4]. Hunter and Riahi [5] used the mean-field approximation to analyze the nonlinear convection in a rotating fluid. They found that the influence of rotation need not always delay the onset of convection, because the heat transfer increase in the intermediate range of rotational parameter. Based on the linear stability analysis, Rudraiah and Chandna [6] analytically showed that the critical Rayleigh number was relatively sensitive to the method and rate of heating, Coriolis force and the nature of the bounding surfaces of the fluid layer. A detailed analysis conducted by Clever and Busse [7] indicated that a higher critical Rayleigh number for the onset of oscillatory motion is found for a system with higher Taylor and Prandtl numbers.

Centrifugally driven thermal convection in a vertical rotating cylinder heated from below was considered by Homsy and Hudson [8]. In that study, both the top and bottom ends of the cylinder were maintained at uniform but different temperatures. By applying boundary layer methods, solutions for both conducting and insulated side walls boundary conditions were obtained on top, bottom, and in the inviscid core of the cylinder, where the axial flow was strongly influenced by the horizontal Ekman layers. In a further study [9], the same authors extended their analysis to indicate the effect of the side wall and heat losses on the Nusselt numbers on both the top and bottom surfaces of the cylinder, where uniform heat flux boundary conditions have been applied. An experimental study of thermal convection in a top heated horizontal rectangular cavity of silicone oil rotating about a vertical axis passing through the geometric center of cavity were carried out by Abell and Hudson [10]. A three-dimensional and unsteady numerical simulation of an

inclined rotating layer, with the rotation vector tilted from the vertical was investigated by Hathaway and Somerville [11]. The tilting of the rotation vector was found to produce a significant change in the flow structure. A combined theoretical, numerical and experimental study of thermal convection in rotating rectangular shallow box heated from below was performed by Buhler and Oertel [12]. They concluded that the roll-cells change their orientation with increasing Taylor number. Moreover, the centrifugal forces dominate in high Prandtl number fluids, while the Coriolis force dominates in low Prandtl number fluids. Unusual flow circulation was experimentally observed by Condie and Griffiths [13] for a horizontal layer of water. Very recently, Lee and Lin [14] and Ker and Lin [15] performed a combined numerical and experimental study of air convection in an inclined rotating cubic cavity. They found that the air flow can be stabilized by the cavity rotation when the rotation rate is low. But at high rotating speed the cavity rotation produced destabilizing effects. Additionally, the inclination of cubic cavity has a significant impact on the flow structure and heat transfer performance.

Study of flow and heat transfer in a closed circular cylinder rotating about its axis is interesting. Experiments for the silicon oil carried out by Hudson et al. [16] and Tang and Hudson [17] indicated that the Nusselt number increases with the rotation rate. Steady axisymmetric numerical simulation was conducted by Chew [18]. The onset of steady natural convection in the confined cylinder was shown by Buell and Catton [19] to be rather sensitive to the lateral thermal boundary condition. Pfotenhauer et al. [20] reported experimental results for the effects of the cylinder geometry on the onset of convection for the low temperature liquid helium. For water subject to the thermal Rayleigh number Ra ranging from 10^6 to 2×10^{11} and Taylor number Ta from 10^6 to 10^{12}, Boubnov and Golitsyn [21] experimentally observed a ring pattern of convection flow resulting from the fluid spin-up and vertex interactions between two adjacent vortices. Kirdyashkin and Distonov [22] found that a periodically changing rotation speed can result in periodic temperature changes throughout the entire liquid layer. Very recently, Ker et al. [23] experimentally examined the

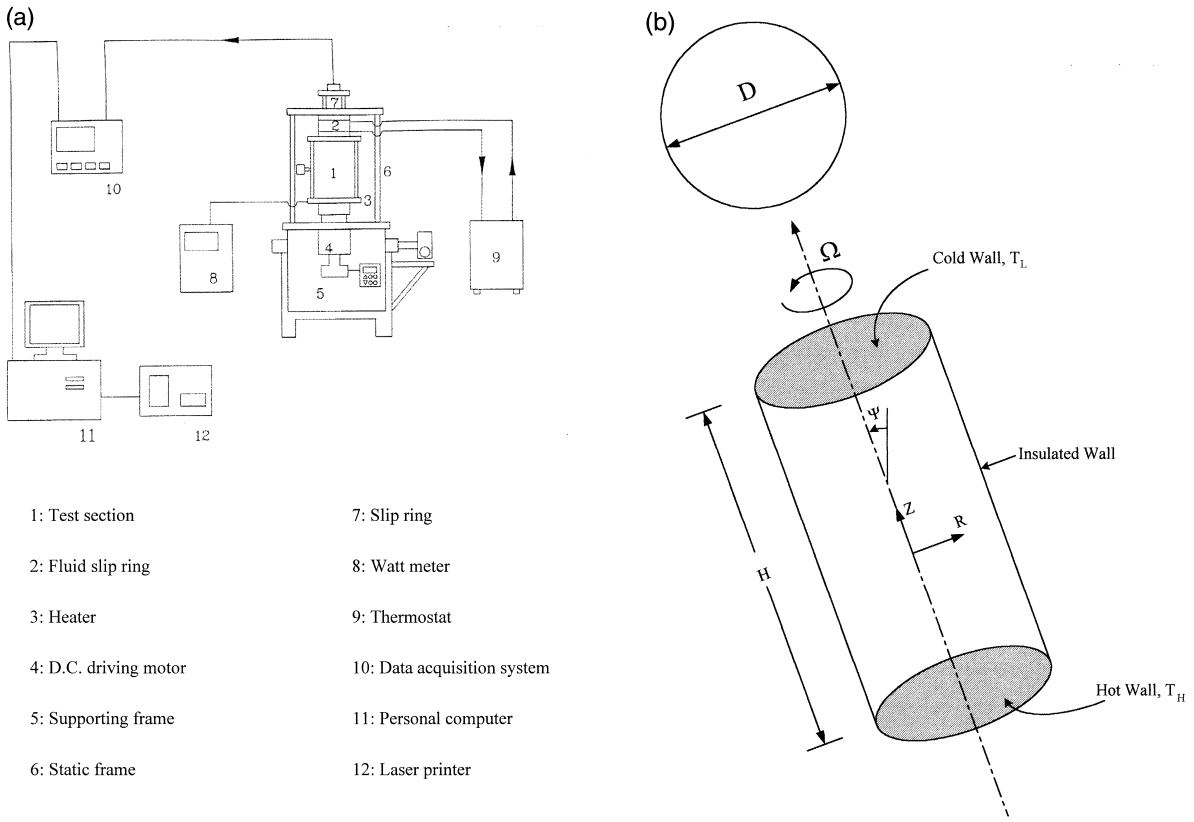

Fig. 1. (a) Schematic diagram of the experimental system. (b) Schematic diagram of the physical model.

unsteady thermal characteristics and rotation-induced stability of air in a heated rotating vertical cylinder.

The above literature survey indicates that the previous studies about the geometry of the cylinders mainly focused on the rotation and the thermal characteristics of a vertical rotating cylinder. But the effects of cylinder inclination on the flow stability and unsteady thermal characteristics are still not well

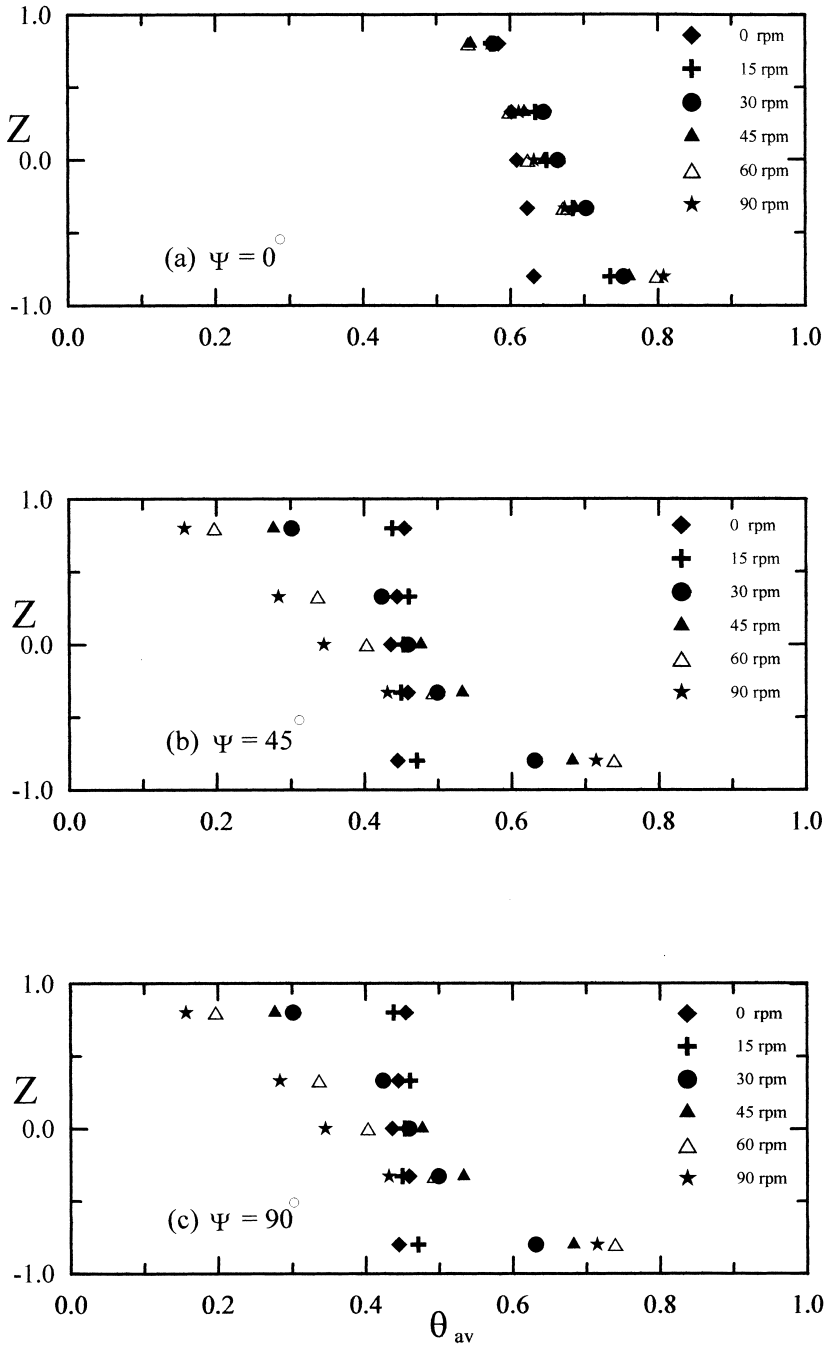

Fig. 2. The time-average temperature distributions along Z-axis $\Delta T = 20°C$ for different rotation rates: (a) $\Psi = 0°$, (b) $\Psi = 45°$, (c) $\Psi = 90°$.

understood. This motivates the present work. The objective of this work is to present a systematic experimental study to examine the thermal characteristics in air-filled heated, inclined cylinders rotating about its axis.

2. Governing parameters

As indicated in the problem formulation [14], the characteristics of flow and heat transfer in a differentially heated rotating cylinder are governed by the Prandtl number Pr, thermal Rayleigh number Ra, Taylor number Ta, rotational Rayleigh number Ra_Ω, and aspect ratio γ. Among these, the thermal Rayleigh number Ra measures the importance of the thermal buoyancy induced by the nonuniformity of temperature in the confined cylinder. The Taylor number Ta characterizes the Coriolis effect or a measure of the relative strength of Coriolis force to viscous forces. The rotational Rayleigh number Ra_Ω measures the significance of the rotation-induced buoyancy effects.

3. Experimental apparatus and techniques

3.1. Apparatus

In the present study, an experimental study of unsteady thermal convection in a differentially heated and inclined rotating cylinder was performed. In a heat transfer experiment, except for a transient test, it may take a long time for the apparatus to reach its steady state. Thus, it may consume lots of time and man power to conduct an experiment in a thermal system. Experimental automation, including sequential control of the experiment, auto-data-acquisition and processing, is of significance in reducing the human errors during the measurements. The experimental system, as schematically shown in Fig. 1(a), is made of four major parts: (1) test section, (2) driving motor

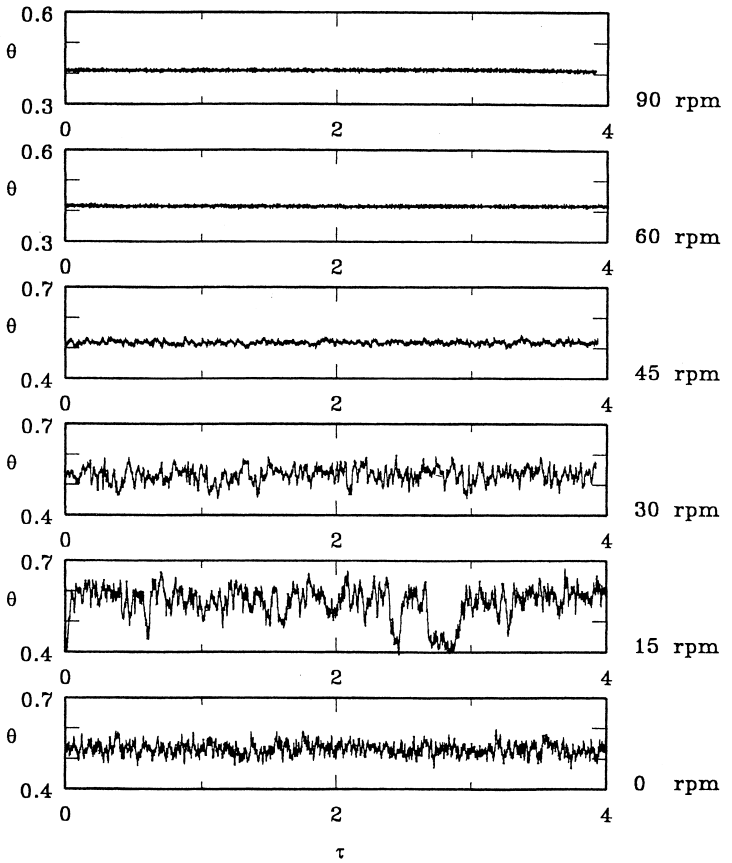

Fig. 3. The time records of air temperature at location $(R, Z) = (0, 0)$ at various rotation rates for $\Psi = 0^\circ$ and $\Delta T = 10^\circ$C.

and speed controller, (3) data acquisition, and (4) thermostat. Fig. 1(a) shows the details of the experimental system.

3.1.1. Test section

The test section fixed on the rotating table is a cylindrical air enclosure 15 cm in diameter and 30 cm height. The physical model of the test section is shown in Fig. 1(b). The cylindrical surface is 1 cm thick clear plexiglas. In order to maintain thermal insulation, a styrofoam insulation with 5.0 cm thickness was used to minimize the heat loss. Both the ends of the cylinder were made of 2 cm thick copper plates which are controlled at uniform, but different temperatures. The high temperature end (bottom wall) was heated electrically with a heater with a total power of 1.0 kW and maintained at a uniform temperature T_H. The power output is presented by a digital wattmeter and controlled by using a digital temperature controller. However, since it was made of 2 cm copper, the desired constant temperature boundary condition was obtained under most conditions. The temperature of the low temperature end (top wall) was kept at T_L and controlled by means of circulating constant temperature coolant through the channel for water circulation. One fluid slip ring was used to allow the coolant to pass from the stationary thermostat to the rotating cylinder. Temperatures of both end surfaces were monitored by three copper–constantan junctions embedded in each of the top and bottom copper surfaces. In this work, the use of thick copper plates of high thermal conductivity is intended to balance the possible temperature gradients and maintain isothermal working surfaces. Additionally, the top and bottom surface temperatures were adjusted during experiments such that the average of two temperatures was equal to ambient temperature T_0. Since physical properties, particularly viscosity, were evaluated at this average temperature, they remain relatively constant throughout, making runs at constant rotational speed equivalent to runs at constant Taylor number *Ta*.

3.1.2. Driving motor and speed controller

The rotating apparatus is driven by a 1 hp dc motor coupled with an inverter by which the rotational speed can be adjusted continuously. The rotating speed is

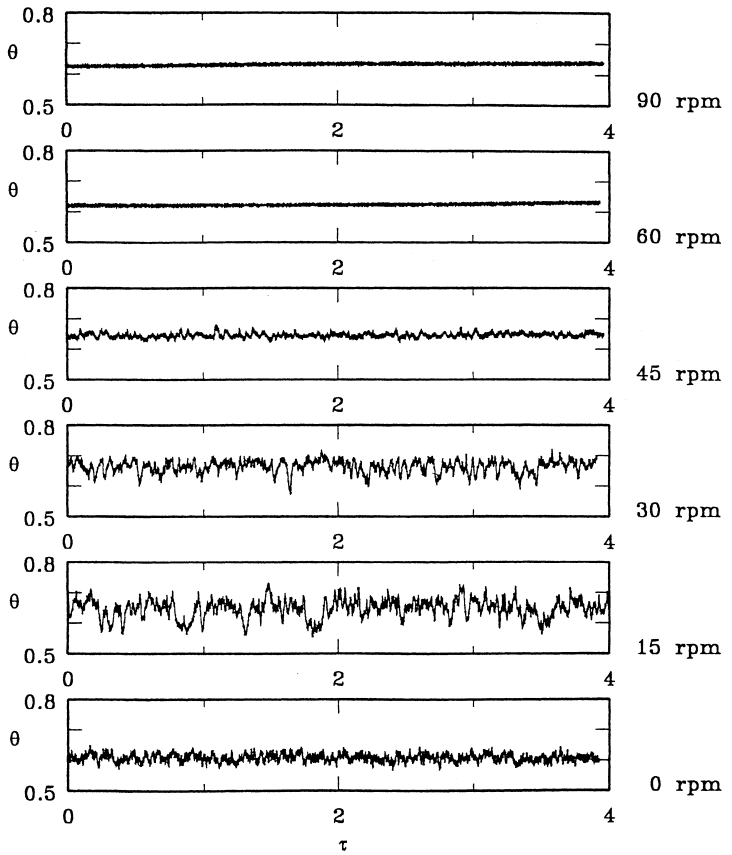

Fig. 4. The time records of air temperature at location $(R, Z) = (0, 0)$ at various rotation rates for $\Psi = 0^\circ$ and $\Delta T = 20^\circ$C.

detected by a photoelectric tachometer. In the present system, the angular velocity ranges from 0 to 90 rpm. For the range of speed used in this work, the error is no more than ± 0.1 rpm. Moreover, the weight of the rotating section acts like a flywheel to stabilize the rotational speed.

3.1.3. Data acquisition

During the test, the voltage signals from the thermocouples were transferred to FLUKE HELIOS Plus 2287A recorder, and then to a personal computer for further data processing. In the present study, data collection was normally started when the flow reaches the steady or statistical state.

3.1.4. Thermostat

In this work, the top end of cylinder was cooled by a flow of water which enters the rotating frame through the fluid slip ring, flows around a chamber in the cooling section, and backs out the thermostat. The thermostat used is the LAUDA RC 25CS compact constant temperature bath with a temperature range of -30–15°C and a resolution of 0.1°C.

3.2. Techniques

3.2.1. Temperature measurements

In the present study, temporal and spatial variations of the air temperature in the rotating cylinder were measured by directly inserting thermocouples of T-type into the cylinder. The T-type thermocouples with diameter 0.0254 mm are fixed at the designated locations by the high performance fine Neoflon threads, which in turn are fixed across the surfaces. Relative to the cylinder diameter (150 mm), size of the inserting thermocouples can be neglected. Therefore, the inserting thermocouples do not affect the flow and thermal fields in the cylinder. Prior to installation, the thermocouples were calibrated by the LAUDA thermostats and high precision liquid-in-glass thermometers. A slipring-brush assembly is used to transfer the thermocouple signals out of the rotating system. The slipring assembly has 20 rings; and its permitted speed for continuous duty is 6000 rpm. All the data are then sent to the personal computer for further data processing. The time history of the data is recorded on the strip chart and also stored in a magnetic disk. Additionally, to check the background noise or slip-ring noise, a temperature measurement about $\Delta T = 0$ was first performed. It was found that the temperature fluctuations at various positions are all below 0.1°C. This justifies that the background or slip-ring noise can be ignored during the experimental period.

3.2.2. Experimental procedure

The variables controlled during experimental work were current to the heater, cooling water temperature, and rotational speed. The current and coolant temperatures were adjusted to give a range of temperature difference from 10 to 20°C. Rotational speed ranges from 0 to 90 rpm.

The test was started by setting the temperature of the thermostat at the predetermined value, and then, setting the appropriate power input such that the bottom temperature can be maintained at desired temperature. The mean value of the hot and cold temperatures was chosen to be equal to the ambient temperature, so that the heat loss from the cylinder to the ambient can be reduced. In the meantime, the cylinder was rotated at the predetermined speed. After the transient stage elapsed, the temporal and spatial variations of the air temperature in the rotating cylinder were measured at the steady or statistical state.

4. Results and discussion

In this work, the effects of rotation on the temporal

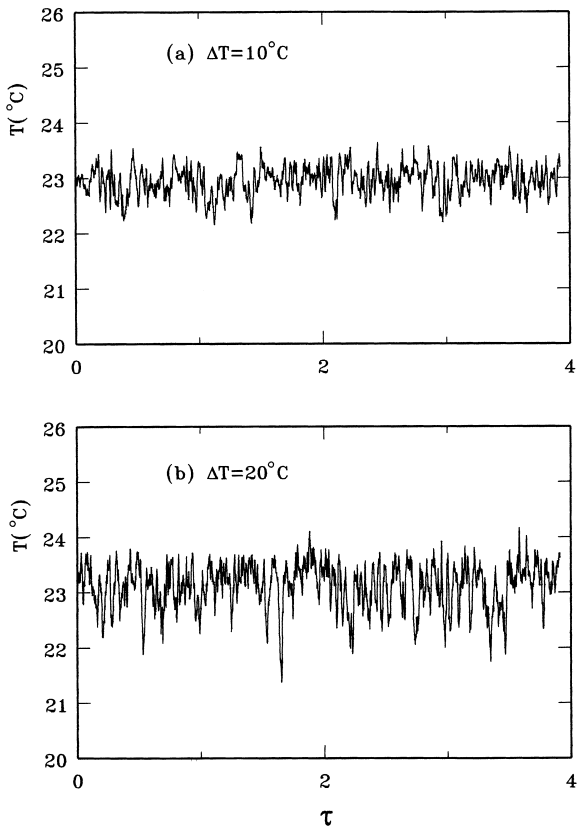

Fig. 5. The time records of air real temperature at location $(R, Z) = (0, 0)$ at rotation rate $\Omega = 30$ rpm for $\Psi = 0^{\circ}$.

variations of air temperature at selected locations in the inclined cylinder were examined. In the following results, only the long term results are presented at which the temperature distribution already reaches steady or statistical state. Attention is focused on the effect of rotation and inclination of the cylinder on the stability of the temperature field.

4.1. Effects of rotation and inclination on time-average temperature

The time-average air temperature variations with the axial coordinate Z $(= z/D)$ along the cylinder axis were measured at different rotation rates Ω and inclined angle Ψ. In this work, the geometrical center of the cylinder was chosen to be the origin of the coordinate system. Fig. 2(a)–(c) present the time-average temperature variations along the Z-axis at different rotation rates Ω and inclined angles Ψ, respectively. An overall inspection of Fig. 2 indicates that for stationary cylinder ($\Omega = 0$ rpm), large temperature gradients exist in the regions near the top and bottom of the cylinder. Outside the regions, the θ_{av} is very uniform for different inclined angles. These phenomena obviously result from the thermal buoyancy driven boundary layer flow in the stationary cylinder at this high thermal Rayleigh number [15,16]. Similar results are also found in the Refs. [15,16]. Close inspection of Fig. 2(a)–(c) discloses that as the cylinder rotates, the temperature gradients near both ends of cylinder are significantly reduced. Additionally, the distributions of the θ_{av} depend on the cylinder inclination. This can be made plausible by noting the fact that for a rise of rotation speed to 30 rpm, the rotation-driven secondary flow strongly interacts with the thermal boundary driven flow which is relative to the inclined angle of the cylinder. Therefore, the thermal characteristics of the air in the cylinders also become sensitive to the cylinder inclination. But as the rotation speed is raised to 60 or 90 rpm, the variations of θ_{av} become linear and depend less on the inclined angle. This is because as the rotation speed is raised to 60 or 90 rpm, the rotation-induced Coriolis

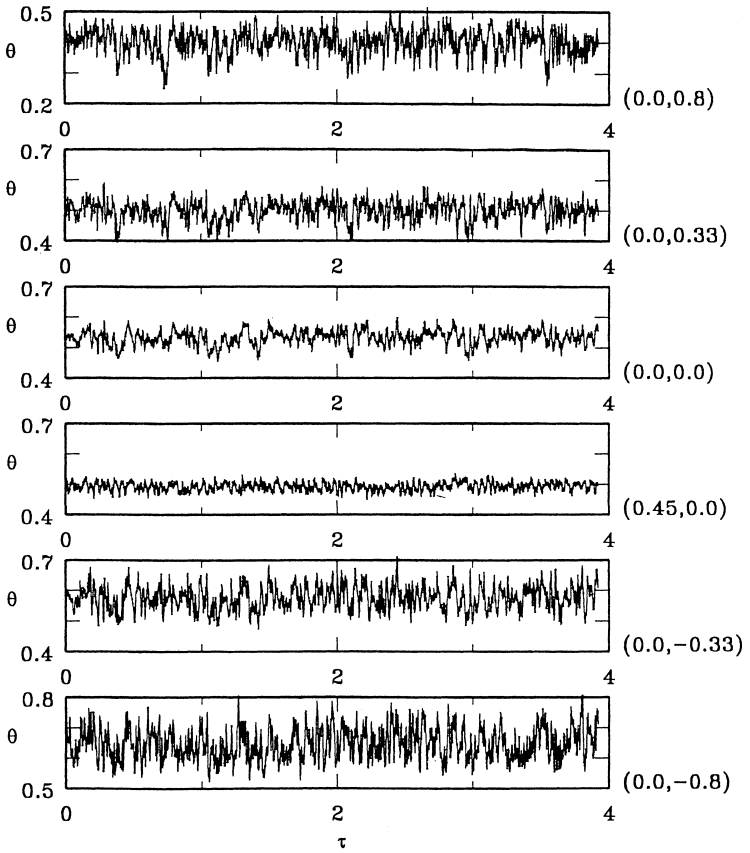

Fig. 6. The time histories of the air temperature at various locations for $\Omega = 30$ rpm and $\Psi = 0^\circ$.

and centrifugal forces dominate over the thermal buoyancy force so that the cylinder inclination produces little influence on the temperature distributions.

4.2. Time records of air temperature

Figs. 3 and 4 show the effects of rotation on the evolution of the air temperature in a vertical cylinder at location $(R, Z) = (0, 0)$ for $\Delta T = 10°C$ ($Ra = 2.3 \times 10^6$) and $\Delta T = 20°C$ ($Ra = 4.6 \times 10^6$). It is interesting to note in Figs. 3 and 4 that when the vertical cylinder is stationary ($\Omega = 0$), the temperature evolution is found to be unsteady with irregular oscillation after initially transient. But as the cylinder is rotated, the rotation effects on the temperature field are complicated. At small rotation rate ($\Omega = 15.0$ rpm), the temperature oscillation is very irregular and high in amplitude. However, as the rotation speed is again raised, rotation-induced destabilizing effect disappears. Only random oscillation at very small amplitude owing to background disturbances were noted at $\Omega = 60.0$ rpm. However, when the rotation speed reaches $\Omega =$ 90.0 rpm, the flow is more stable. It is also clear that for a higher temperature difference ΔT, the thermal buoyancy-driven flow becomes unstable. In Figs. 3 and 4, the dimensionless temperature fluctuations seem to be smaller for a system with a higher ΔT. As shown in Fig. 5, the real temperature fluctuations of Figs. 3 and 4 at $\Omega = 30.0$ rpm indicates that higher real temperature fluctuations are noted for $\Delta T = 20°$C. A larger amplitude irregular temperature is detected for a higher ΔT at $\Omega = 0$. Clearly, this is due to a greater thermal buoyancy effect for a system with a higher temperature difference ΔT. Additionally, a higher rotation rate is needed to destabilize the flow field for a system with a higher ΔT.

As mentioned above, the resulting flow in a stationary cylinder is time oscillatory at a larger τ. But in the presence of rotation $\Omega < 30$ rpm), the flow is found to become more unstable with the oscillation amplitude increased noticeably. This implies that the combined effects of rotation-induced Coriolis and centrifugal forces would destabilize the flow field. But as $\Omega \geq 30$ rpm, the oscillation in temperature dis-

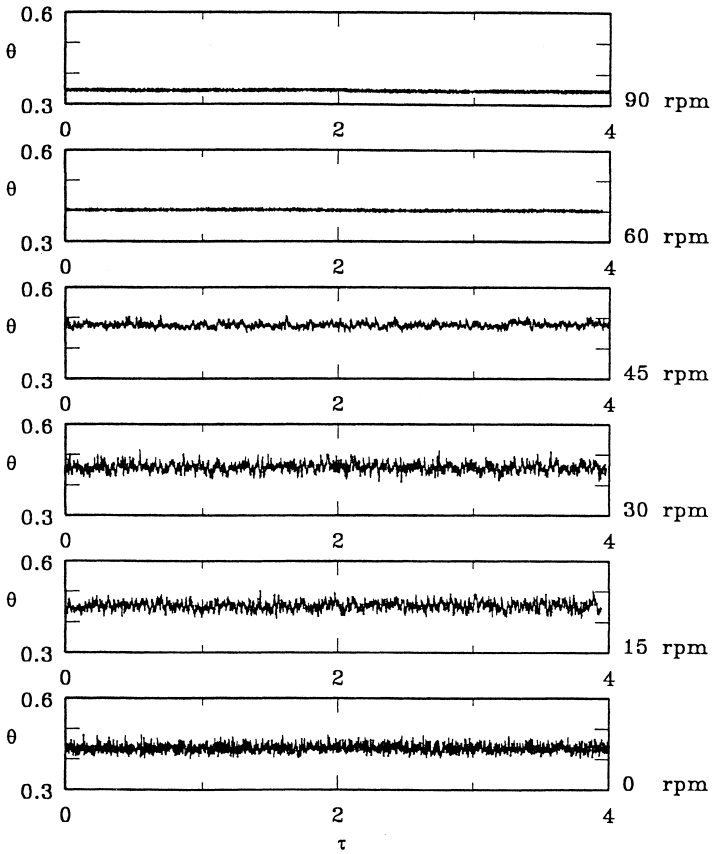

Fig. 7. The time records of air temperature at location $(R, Z) = (0, 0)$ at various rotation rates for $\Psi = 45°$ and $\Delta T = 20°$C.

tribution is decreased with an increase in the rotation speed Ω.

The time histories of the air temperature in a vertical cylinder at various locations for $\Delta T = 20°C$ at fixed rotation speed are presented in Fig. 6. Checking the evolution of the air temperature at six different locations indicates that the temperature distributions oscillate nearly at the same frequency, but in different amplitudes. But a careful inspection on Fig. 6 discloses that a smaller temperature oscillation is noted for the results closer to the insulation cylinder wall due to the wall damping effect.

The other major parameter of concern is the inclined angle of rotating cylinder Ψ. Figs. 7 and 8 show the temperature variations at the cylinder center with various rotation rates for $\Psi = 45$ and 90°, respectively. It is found that at the same rotation rate Ω, the flow becomes more stable as the inclination of the cylinder increases. In fact, at the inclination angle $\Psi \geq 60°$, the temperature evolution is stable over the ranges of rotation rate Ω from 0 to 90 rpm. This can be clearly seen in Fig. 9.

4.3. Energy of temperature oscillation

To further illustrate the characteristics of the temperature oscillation, the results of time-average energy of the dimensionless air temperature fluctuation $\overline{(\theta - \theta_{av})^2}$ are presented in Fig. 9 at different rotation rates Ω and inclined angle Ψ. It is clear in Fig. 9 that the value of $\overline{(\theta - \theta_{av})^2}$ decreases with the increase in inclined angle Ψ. Additionally, for $\Omega \geq 30$ rpm, the fluctuation energy decreases with the rotation speed. This implies that at $\Omega \geq 30$ rpm, the flow is stabilized by the cylinder rotation. However for $\Omega < 30$ rpm, the effects of rotation on the flow field depends on the inclined angle Ψ.

5. Concluding remarks

The thermal characteristics of the air in differentially heated, rotating, inclined cylinders were examined experimentally, in details. In this work, the effects of rotation rate Ω and cylinder inclination Ψ on the time-

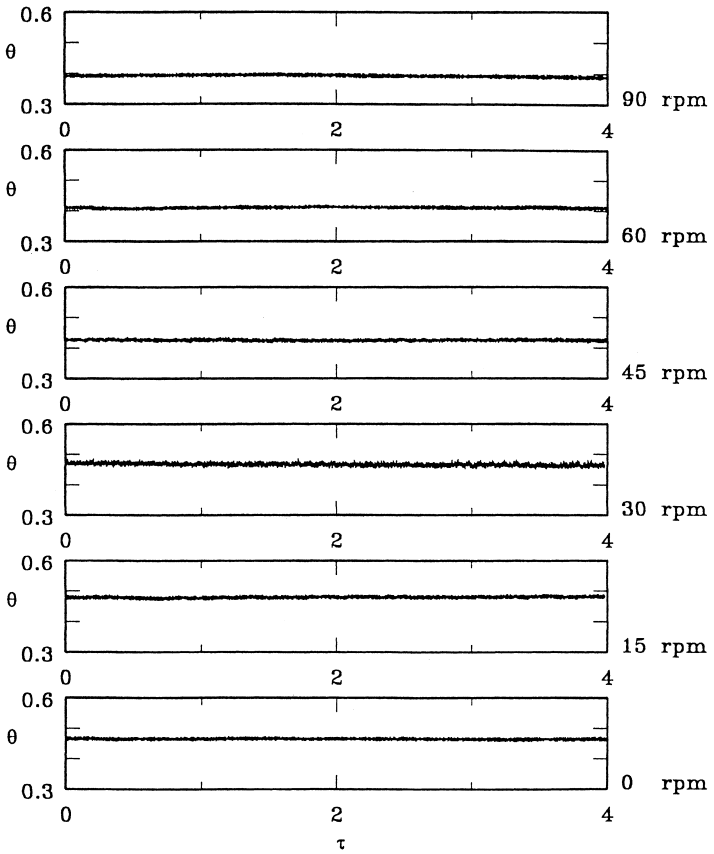

Fig. 8. The time records of air temperature at location $(R, Z) = (0, 0)$ at various rotation rates for $\Psi = 90°$ and $\Delta T = 20°C$.

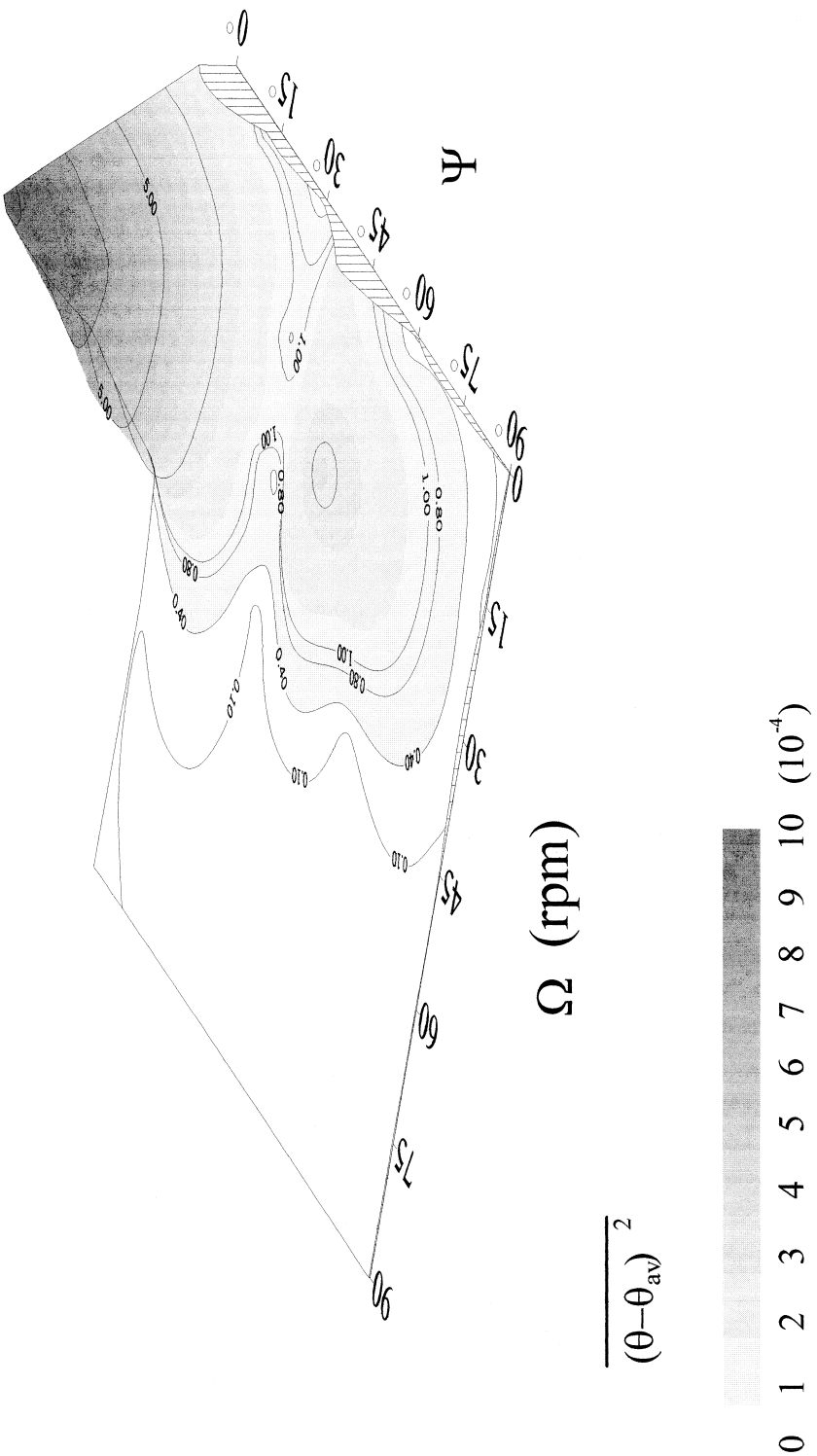

Fig. 9. Variations of time-average energy of temperature fluctuation with rotation rate Ω and inclined angle Ψ.

average temperature, evolution of temperature and energy of temperature fluctuation can be clearly seen from these results. The major findings are summarized below:

1. For stationary cylinder ($\Omega = 0$ rpm), the distributions of the time-average temperature θ_{av} in the Z-axis are nearly uniform for various inclined angles Ψ.
2. For rotating cylinder, the distributions of θ_{av} depend on the inclined angle when the rotation rate $\Omega \leq 30$ rpm. But as $\Omega \geq 60$ rpm, the results of θ_{av} depend less on the cylinder inclination.
3. For stationary cylinder, the temperature evolution is found to be unsteady with irregular oscillation after initially transient.
4. As the cylinder is rotated with angular speed $\Omega =$ 15.0 rpm, the temperature oscillation is very irregular and of high amplitude. But as the rotation speed is raised ($\Omega \geq 60$ rpm), rotation-induced destabilizing effect disappears.
5. A higher rotation rate is needed to stabilize the flow field for a system with a higher temperature difference ΔT.

Acknowledgements

The financial support of this work by the National Science Council of Taiwan, R.O.C., through the contract NSC 87-2212-E211-006 is gratefully acknowledged. Additionally, the valuable suggestions from Dr. Y.T. Ker are very much appreciated.

References

[1] P.P. Niller, F.E. Bisshopp, On the influence of Coriolis force on onset of thermal convection, J. Fluid Mechanics 22 (1965) 753–761.
[2] G. Veronis, Large-amplitude Benard convection in a rotating fluid, J. Fluid Mechanics 31 (1968) 113–139.
[3] G. Kuppers, D. Loetz, Transient from laminar convection to thermal turbulence in a rotating fluid layer, J. Fluid Mechanics 35 (1969) 609–620.
[4] H.T. Rossby, A study of Benard convection with and without rotation, J. Fluid Mechanics 36 (1969) 309–335.
[5] C. Hunter, N. Riahi, Nonlinear convection in a rotating fluid, J. Fluid Mechanics 72 (1975) 433–454.
[6] N. Rudraiah, O.P. Chandna, Effects of Coriolis force and nonuniform temperature gradient on the Rayleigh–Benard convection, Can. J. Phys 64 (1986) 90–99.
[7] R.M. Clever, F.H. Busse, Nonlinear properties of convection rolls in a horizontal layer rotating about a vertical axis, J. Fluid Mechanics 94 (1979) 609–627.
[8] G.M. Homsy, J.L. Hudson, Centrifugal driven thermal convection in a rotating cylinder, J. Fluid Mechanics 35 (1969) 33–52.
[9] G.M. Homsy, J.L. Hudsom, Heat transfer in a rotating cylinder of fluid heated from above, Int. J. Heat Mass Transfer 14 (1971) 1149–1159.
[10] S. Abell, J.L. Hudson, An experimental study of centrifugally driven free convection in rectangular cavity, Int. J. Heat Mass Transfer 18 (1975) 1415–1423.
[11] D.H. Hathaway, R.C.J. Somerville, Three-dimensional simulations of convection in layers with tilted rotation vectors, J. Fluid Mechanics 126 (1983) 75–89.
[12] K. Buhler, H. Oertel, Thermal cellular convection in rotating rectangular boxes, J. Fluid Mechanics 114 (1982) 261–282.
[13] S.A. Condie, R.W. Criffiths, Convection in rotating cavity: modeling ocean circulation, J. Fluid Mechanics 207 (1989) 453–474.
[14] T.L. Lee, T.F. Lin, Transient three-dimensional convection of air in a differentially heated rotating cubic cavity, Int. J. Heat Mass Transfer 39 (1996) 1243–1255.
[15] Y.T. Ker, T.F. Lin, A combined numerical and experimental study of air convection in a differentially heated rotating cubic cavity, Int. J. Heat Mass Transfer 39 (1996) 3193–3210.
[16] J.L. Hudson, D. Tang, S. Abell, Experiments on centrifugal driven thermal convection in a rotating cylinder, J. Fluid Mechanics 86 (1978) 147–159.
[17] D. Tang, J.L. Hudson, Experiments on a rotating fluid heated from below, Int. J. Heat Mass Transfer 26 (1983) 943–949.
[18] J.W. Chew, Computation of convective laminar flow in rotating cavities, J. Fluid Mechanics 153 (1995) 339–360.
[19] J.C. Buell, I. Catton, Effect of rotation on the stability of a bounded cylindrical layer of fluid heated from below, Phys. Fluids 26 (1983) 892–896.
[20] J.M. Pfotenhauer, J.J. Niemela, R.J. Donnelly, Stability and heat transfer of rotating criogens, part 3, effects of finite cylindrical geometry and rotation on the onset of convection, J. Fluid Mechanics 175 (1987) 85–96.
[21] B.M. Boubnov, G.S. Golitsyn, Experimental study of convective structures in rotating fluid, J. Fluid Mechanics 167 (1986) 503–531.
[22] A.G. Kirdyashkin, V.E. Distonov, Hydrodynamics and heat transfer in a vertical cylinder exposed to periodically varying centrifugal forces (accelerated crucible rotating technique), Int. J. Heat Mass Transfer 33 (1990) 1397–1415.
[23] Y.T. Ker, Y.H. Li, T.F. Lin, Experimental study of unsteady thermal characteristics and rotation induced stabilization of air convection in a bottom heated rotating vertical cylinder, Int. J. Heat Mass Transfer 41 (1998) 1445–1458.